IOP Conf. Series: Materials Science and Engineering **444** (2018) 082002 doi:10.1088/1757-899X/444/8/082002

Working fluid selection procedure for ORC-based systems coupled with internal combustion engines driving electrical generators

H Pop[1], V Apostol[1], V Bădescu[1], M H K Aboaltabooq[2], T Prisecaru[1], E Pop[1] M Prisecaru[1] and D Taban[1]

[1]Department of Thermodynamics, Engines, Thermal and Refrigeration Equipment, Faculty of Mechanical Engineering and Mechatronics, University POLITEHNICA of Bucharest, Spl. Independentei 313, Bucharest 060042, Romania
[2]AL-Furat Al-Awsat Technical University, Technical College Najaf

E-mail: valentin.apostol@magr.ro

Abstract. The paper deals with waste heat recovery (WHR) from internal combustion engines (ICE) using organic Rankine cycle based systems (ORC), due to its ability to operate with moderate temperature differences. The waste heat source is flue gas from an ICE that drives a stationary electric generator. The configuration of the ORC system is the basic one. The mathematical modelling of the ICE-ORC system is a continuation of previous work conducted by the authors and has been validated by using as input, data from other similar papers. The results are in good agreement. The mathematical model has also been used as part of a working fluid selection procedure for the ORC system. The working fluid selection procedure is based on screening fifteen candidate fluids and selecting the most suitable ones by using three criteria: environmental, safety and technical. A discussion about the type of working fluid is conducted. The screened working fluids are R134a, R236fa, R245fa, R1234yf, R1234ze, R290, R600, R600a, pentane, hexane, benzene, toluene, RC318, HFE7100 and HFE7500. Results point out that the most suitable candidates are R134a, R1234yf and R1234ze. In future work, specific results will be presented for this three selected fluids.

1. Introduction

Waste heat recovery (WHR) from the internal combustion engine (ICE) in a useful form of energy is a challenge nowadays given the context of escalating fuel prices and future carbon dioxide and NOx limits. For over 100 years, ICE has been and continues to be the primary power source for land and maritime transport, but also the main source of mechanical and electrical power generation in isolated areas lacking infrastructure of electrification networks. Over time, high fuel costs and oil dependence have prompted the invention of increasingly complex engine models to reduce fuel consumption. Moreover, the ever-stricter emissions regulations oblige engine manufacturers to limit combustion temperatures and pressures by curbing potential efficiency gains [1]. Nowadays, about 35% -40% of the combustion energy in ICE is converted into useful mechanical work, and the remainder is residual heat expelled to the environment through combustion gases and engine cooling systems. Recovery and use of this waste heat saves fossil fuels and reduces the amount of greenhouse gases released into the environment [2]. The two primary sources of residual heat from an ICE are the resulting combustion gases (with a medium temperature level) and the engine coolant (with a lower temperature level). Both

Content from this work may be used under the terms of the Creative Commons Attribution 3.0 licence. Any further distribution of this work must maintain attribution to the author(s) and the title of the work, journal citation and DOI.
Published under licence by IOP Publishing Ltd

primary engine sources listed above having similar energy content and higher exhaust temperature are more thermodynamically attractive when viewed from the perspective of exergy analysis. A review of the literature on WHR shows that ICE can produce heat with sufficient exergy to justify the implementation of a secondary cycle [1]. Many researchers recognize that the recovery of engine exhaust heat has the potential to reduce fuel consumption without increasing emissions, and recent technological advances have made these systems viable and cost-effective. Most studies have focused on choosing a Rankine or Rankine organic (ORC) cycle for WHR due to its ability to operate with moderate temperature differences. It is also possible to perform WHR using other thermodynamic cycles. Among the most common methods we mention: the Brayton cycle, which requires only three components, the Stirling engine cycle, which includes a closed system consisting of a regenerator and a cylinder containing both the piston and the power piston, or the Kalina cycle, which is a configuration parallel between an ORC with the addition of an absorbent and a reservoir [1]. This cycle uses a variable mixture of ammonia and water as working fluid. Similarly, supercritical carbon dioxide systems as working fluid have attracted attention in various WHR applications. While most WHR research focuses on thermodynamic cycles, due to technological advances over the past decade, thermoelectric devices provide a unique alternative because they directly convert heat into electricity [2].

The present paper focuses on heat recovery from the flue gas of ICE by means of an ORC-based system. Present work is a continuation of a previous work [3] and it focuses mainly on developing the mathematical model, validation of the mathematical model and presentation of a working fluid selection procedure.

2. ORC-based systems for heat recovery

Several schemes of ORC-based systems for heat recovery from Internal Combustion engines (ICEs) are of practical interest and can be implemented in real life [4]. One of them is shown here, as illustration. It involves only recovery of heat from flue gas and requires the smaller amount of investments.

In this configuration, the ORC-based heat recovery system is composed of expander, condenser, evaporator (heat recovery unit), working fluid pump and other auxiliary equipment (Figure 1). The heat source, such as flue gas removed from the internal combustion engines, is acting in the evaporator (process 1-2), where the working fluid is evaporated (boils), then delivered to the expander inlet (process 2-3). The working fluid drives the expander to generate work (process 3-4), associated with pressure and temperature decrease. The work is converted into electricity using an electric generator. The low pressure and temperature working fluid is cooled to liquid phase when passing through the condenser (process 4-1). The working fluid pump transports the liquid working fluid back into the evaporator (process 1-2), to absorb heat, then the above process repeats.

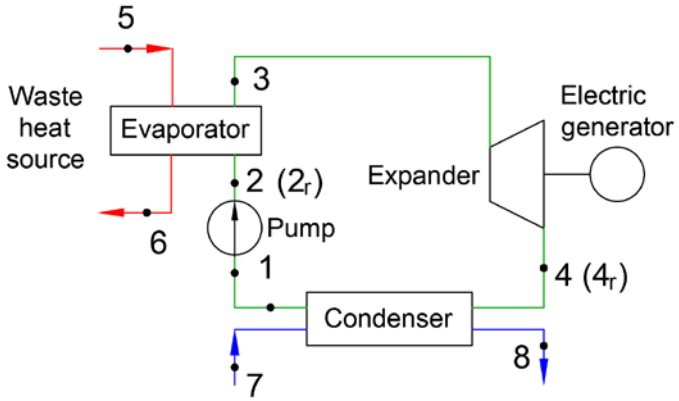

Figure 1. General scheme of an ORC-based heat recovery system.

The thermodynamic cycle of the ORC-based system configuration from Figure 1 is presented in Figure 2 in three different situations a) for "wet" working fluids, b) for "isentropic" working fluids and c) for "dry" working fluids. The working fluids for ORC-based systems can be divided into three main groups: "wet", "isentropic" and "dry". The differences between them are explained in section 5. The shape of the saturation curves from Figure 2 a), b) and c) are generated using the Engineering Equation Solver (EES) [5] as follows: for Figure 2 a) R134a "wet" fluid is used, for Figure 2 b) R245fa "isentropic" fluid is used and for Figure 2 b) toluene "dry" fluid is used. For all three cases presented in Figure 2 a), b) and c) the thermodynamic processes that occur and are considered in this paper are: 1-2 isentropic process across pump or 1-2r real process across pump; 2 (2r)-3 heat absorption process in the evaporator which can be divided into three different processes: 2 (2r)-2sat preheating process, 2sat-3sat boiling (evaporation) process and 3sat-3 superheating process; 3-4 isentropic expansion process in the expander or 3-4r real expansion process in the expander and 4 (4r) – 1 heat rejection process in the condenser which can be divided into two different processes: 4 (4r) - 5sat desuperheating process and 5sat-1 condensation process. Also, in Figure 2 a), b) and c) state 8 corresponds to the flue gas inlet in the evaporator, state 6 corresponds to the flue gas outlet of the evaporator, state 9 is the state of the flue gas in the evaporator for which a corresponding saturated dry vapor state for the working fluid in ORC-based system is achieved, state 10 is the state of the flue gas in the evaporator for which a corresponding saturated liquid state for the working fluid in ORC-based system is achieved, state 7 is the condenser cooling water state at the condenser inlet, state 8 is the condenser cooling water state at the condenser outlet and state 11 which is the condenser cooling water state for which a corresponding saturated dry vapor state for the working fluid in the ORC-based system is achieved.

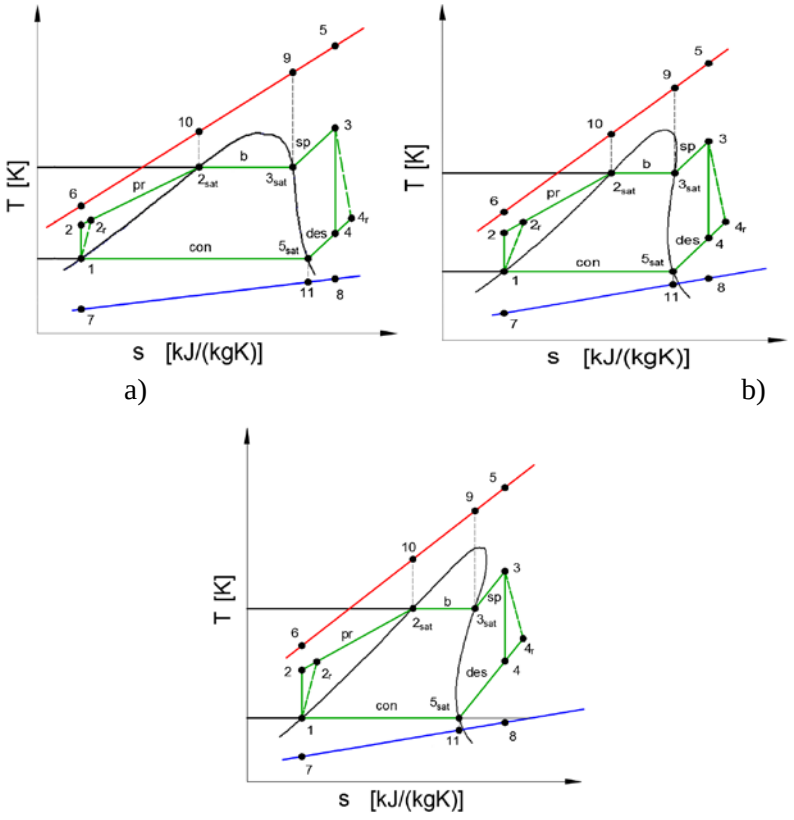

Figure 2. The thermodynamic cycle in T-s coordinates for the ORC-based system configuration presented in Figure 1 a) for "wet" working fluids, b) for "isentropic" working fluids and c) for "dry" working fluids.

3. Mathematical modelling of the ORC-based system

The model of the ORC-based system is structured into several sub-models. It is based on balance mass and energy equations for all system components (evaporator, expander, condenser and pump). Appropriate heat transfer relationships are used for these components and performance indicators are defined. The assumptions adopted for the development of the mathematical model are as follows: (i) negligible heat loss in pipes and equipment; (ii) negligible pressure drops in pipes and equipment; (iii) flue gas is non-condensable; (iv) steady state operation.

The mathematical sub-models for the pump, evaporator, expander and condenser are presented in detail in a previous work conducted by the authors [3]. However, for the ease of understanding some elements of the sub-models presented in [3] are resumed next. Also new elements like irreversibility analysis are presented.

3.1. Mathematical sub-model for the pump

During the real process inside the pump (1-2r), the working fluid pressure increases form condensing pressure to evaporating pressure based on a specific power supply. The real power supply at the pump level which is enables the working fluid to describe the thermodynamic cycle presented in Figure 2 can be computed using the following relationship:

$$P_{pump,real} = \frac{P_{pump,ideal}}{\eta_p} = \frac{\dot{m}_{ref}\left(h_1 - h_2\right)}{\eta_p} = \dot{m}_{ref}\left(h_1 - h_{2r}\right). \quad (1)$$

In relationship (1) $P_{pump,real}$ stands for the real pump power supply, $P_{pump,ideal}$ stands for the theoretical (ideal) pump power supply, $\dot{m}_{ref}$ is the working fluid mass flow rate, h_1 is the enthalpy of the working fluid at the pump inlet, h_2 is the enthalpy of the working fluid at the pump outlet for the ideal case, h_{2r} is the enthalpy of the working fluid at the pump outlet for the real case and η_p is the efficiency of the pump.

From relationship (1) the value for the working fluid enthalpy at the pump outlet corresponding to the real case (h_{2r}) can be computed as follows:

$$h_{2r} = h_1 + \frac{h_2 - h_1}{\eta_P}. \quad (2)$$

The equation of the exergy destruction in the pump (the irreversibility) is:

$$\dot{I}_{pump} = \dot{m}_{ref} T_{amb}\left[\left(s_{2r} - s_1\right)\right]. \quad (3)$$

where s_1 and s_{2r} are the specific entropies of the working fluid at the inlet and outlet of the pump for the real case, respectively.

3.2. Mathematical sub-model for the evaporator

After the working fluid exits the pump, it enters into the evaporator where it absorbs heat from the heat source which in the present case is flue gas from an ICE. As presented in Figure 3 and in correlation with Figure 2, the evaporator can be divided into three zones a preheater zone (pr) where the working fluid is preheated from state 2r (pump outlet) to state 2sat, a boiler (b) zone where the working fluid boils (evaporates) and changes its state from 2sat to 3sat and a superheated (sp) zone where a superheating process from state 3sat to state 3 takes place.

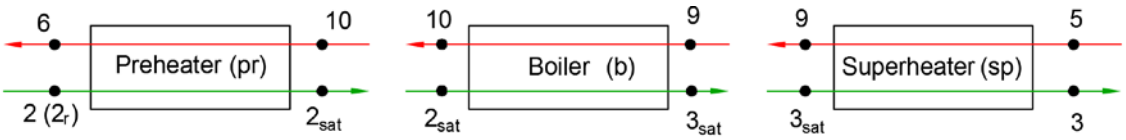

Figure 3. The three zones of the evaporator.

The outlet state 3 of the working fluid from the evaporator can be determined as follows:

$$T_3 = T_{3sat} + \Delta T_{sp}. \tag{4}$$

In relationship (4), ΔT_{sp} is the superheating increment in the evaporator.

In the evaporator, during the heat absorption process there are four temperature differences between the flue gas and working fluid as follows: $\Delta T_{in} = T_5 - T_3$, $\Delta T_1 = T_9 - T_{3sat}$, $\Delta T_2 = T_{10} - T_{2sat}$ and $\Delta T_{out} = T_6 - T_{2r}$. Using the work conducted in [3] the heat transfer areas for the preheater (A_{pr}), boiler (A_b), superheater (A_{sp}) and the overall heat transfer area for the evaporator can be computed (A_{evap}).

The exergy destruction in the evaporator can be expressed as follows [6]:

$$\dot{I}_{evap} = \dot{m}_{ref} T_{amb} \left[(s_3 - s_{2r}) - \frac{(h_3 - h_{2r})}{T_H} \right]. \tag{5}$$

In relationship (5), T_{amb} is the ambient temperature, s_3 is the specific entropy of the working fluid in state 3, h_3 is the enthalpy of the working fluid in state 3 and T_H is the temperature of the heat source and can be computed as the mean thermodynamic temperature corresponding to the cooling process of the flue gas in the evaporator (process 5-6 from Figure 2):

$$T_H = \frac{\dot{Q}_{source}}{\dot{S}_{source}} = \frac{\dot{m}_g (h_5 - h_6)}{\dot{m}_g (s_5 - s_6)}. \tag{6}$$

Where $\dot{Q}_{source}$ is the heat flux transferred in the evaporator to the ORC-based system working fluid by the flue gases (assuming that there are no heat losses to the surroundings), $\dot{S}_{source}$ is the entropy flux corresponding to the flue gas cooling process, $\dot{m}_g$ is the flue gas mass flow rate, h_5 is the enthalpy of the flue gas at the evaporator inlet, h_6 is the enthalpy of the flue gas at the evaporator outlet, s_5 is the entropy of the flue gas at the evaporator inlet and s_6 is the entropy of the flue gas at the evaporator outlet.

3.3. Mathematical sub-model for the expander

Through the real expansion process 3-4r in the expander, the energy of the working fluid is converted into work [3,7] that finally leads to the mechanical power output:

$$P_{expander,real} = P_{expander,ideal} \eta_{exp} = \dot{m}_{ref} (h_3 - h_4) \eta_{exp} = \dot{m}_{ref} (h_3 - h_{4r}). \tag{7}$$

In relationship (7), $P_{expander,real}$ is the real power output of the expander, $P_{expander,ideal}$ is the expander power output in the ideal case, η_{exp} is the expander efficiency, h_4 is the enthalpy of the working fluid at the expander outlet for ideal case and h_{4r} is the enthalpy of the working fluid at the expander outlet for the real case.

The enthalpy of the working fluid at the expander outlet (state 4r from Figure 2) can be computed as follows:

$$h_{4r} = h_3 - (h_3 - h_4) \cdot \eta_{exp}. \tag{8}$$

The exergy destruction in the expander can be expressed as:

$$\dot{I}_{exp} = \dot{m}_{ref} T_{amb} \left[(s_{4r} - s_3) \right]. \tag{9}$$

where s_{4r} is the entropy of the working fluid at the outlet of the expander for the real case.

3.4. Mathematical sub-model for the condenser

After the expander, the working fluid enters the condenser where it rejects heat to the cooling water, in the present case. As shown in Figure 4 and in correlation with Figure 2, the condenser can be divided into two zones, a desuperheating zone (des) where the working fluid cools from superheated vapor state 4 (4r) to dry saturated vapor state 5sat and the condensation zone (con) where the working fluid condensates and it changes its state from 5sat to 1.

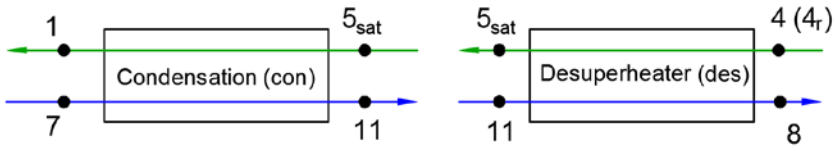

Figure 4. The two zones of the condenser.

In the condenser, during the heat rejection process there are three temperature differences between the working fluid and cooling water: $\Delta T_{conin} = T_{4r} - T_8$, $\Delta T_{con1} = T_{5sat} - T_{11}$, and $\Delta T_{conout} = T_1 - T_7$.

Using the work conducted in [3] the heat transfer areas for the desuperheater zone (A_{des}), condensation zone (A_{con}) and the overall heat transfer area for the condenser can be computed ($A_{condenser}$).

The exergy destruction in the condenser is expressed as:

$$\dot{I}_{con} = \dot{m}_{ref} T_{amb} \left[(s_1 - s_{4r}) - \frac{(h_1 - h_{4r})}{T_L} \right]. \tag{10}$$

In relationship (10), s_1 is the entropy of the working fluid at the condenser outlet and T_L is the mean thermodynamic temperature of the water in the heating process 7-8 that take place in the condenser and it can be computed as follows:

$$T_L = \frac{\dot{Q}_{rejected}}{\dot{S}_w} = \frac{\dot{m}_w (h_8 - h_7)}{\dot{m}_w (s_8 - s_7)}. \tag{11}$$

Where $\dot{Q}_{rejected}$ is the heat flux transferred by the working fluid to the cooling water (assuming again that there are no heat losses to the surroundings), $\dot{S}_w$ is the entropy flux corresponding to the heating process of the water in the condenser, $\dot{m}_w$ is the condenser cooling water mass flow rate, h_8 is the enthalpy of the cooling water at the condenser outlet, h_7 is the enthalpy of the cooling water at the condenser inlet, s_8 is the entropy of the cooling water at the condenser outlet and s_7 is the entropy of the cooling water at the condenser inlet.

3.5. Mathematical model for the overall ORC-based system

The heat flux absorbed in the evaporator by the ORC-based system working fluid, if the heat loss to the surroundings is neglected, can be expressed as:

$$\dot{Q}_{source} = \dot{m}_{ref} (h_3 - h_{2r}). \tag{12}$$

Also, $\dot{Q}_{source}$ can be expressed as a sum of the heat fluxes absorbed in the preheater ($\dot{Q}_{pr}$), boiler ($\dot{Q}_b$) and superheater ($\dot{Q}_{sp}$) as follows:

$$\dot{Q}_{source} = \dot{Q}_{pr} + \dot{Q}_b + \dot{Q}_{sp}\,. \tag{13}$$

The heat fluxes $\dot{Q}_{pr}$, $\dot{Q}_b$ and $\dot{Q}_{sp}$ can be computed using relationships (14-16):

$$\dot{Q}_{pr} = \dot{m}_{ref}\left(h_{2sat} - h_{2r}\right). \tag{14}$$

$$\dot{Q}_b = \dot{m}_{ref}\left(h_{3sat} - h_{2sat}\right). \tag{15}$$

$$\dot{Q}_b = \dot{m}_{ref}\left(h_3 - h_{3sat}\right). \tag{16}$$

The net power output of the ORC-based system can be computed using relationship (17):

$$P_{net,ORC} = P_{expander,real} - P_{pump,real}\,. \tag{17}$$

The thermal efficiency of the ORC-based system can be determined as follows:

$$\eta_{th,ORC} = \frac{P_{net,ORC}}{\dot{Q}_{source}}\,. \tag{18}$$

The total exergy destruction in the ORC-based system is obtained from a summation of the exergy destruction inside all parts of the system:

$$\dot{I}_{total} = \dot{I}_{pump} + \dot{I}_{evap} + \dot{I}_{exp} + \dot{I}_{con}\,. \tag{19}$$

The exergy efficiency (the second law efficiency) is defined by the ratio of the expander output power and the summation of the expander output power and the total exergy destruction of the cycle:

$$\eta_{II,ORC} = \frac{P_{exp,real}}{P_{exp,real} + \dot{I}_{total}}. \tag{20}$$

4. Mathematical model validation

Based on a previous work conducted by the authors [3] and the mathematical modelling described in Section 3 a program has been developed in Engineering Equation Solver - EES [5]. The flow chart of the program is presented in Figure 5.

The results obtained the program developed in EES have been validated using the work conducted in [8] and [9]. Both [8] and [9] refer to waste heat recovery from ICE by means of ORC-based systems. The program developed in EES has been used for the input data corresponding to [8] and the results are presented in Table 1 for R245fa and R134a as working fluids for the ORC-based system. The input data used is: flue gas composition in terms of mass fractions – $m_{CO2} = 15.10\,\%$, $m_{H2O} = 5.37\,\%$, $m_{N2} = 73.04\,\%$, $m_{O2} = 6.49\,\%$, temperature of the flue gas at the evaporator inlet $T_5 = 792.15\ K$, temperature of the flue gas at the evaporator outlet (form the condition of avoiding condensation) $T_6 = 393.15\ K$, flue gas mass flow rate $\dot{m}_g = 990.79\ kg/h$, temperature of the ORC-based system working fluid at the expander inlet $T_3 = 523.15\ K$, evaporating pressure $p_{evap} = 3000\ kPa$, condensing temperature $T_{con} = 308.15\ K$, expander efficiency $\eta_{exp} = 0.7$, pump efficiency $\eta_p = 0.8$. The results that are compared in Table 1 are: thermal efficiency of the ORC-based

system $\eta_{th,ORC}\,[-]$, expansion ratio $v_{4r}/v_3\,[-]$ and total heat transfer area (evaporator plus condenser) per net power output of the ORC-based system $A_{tot}/P_{net,ORC}\,[m^2/kW]$.

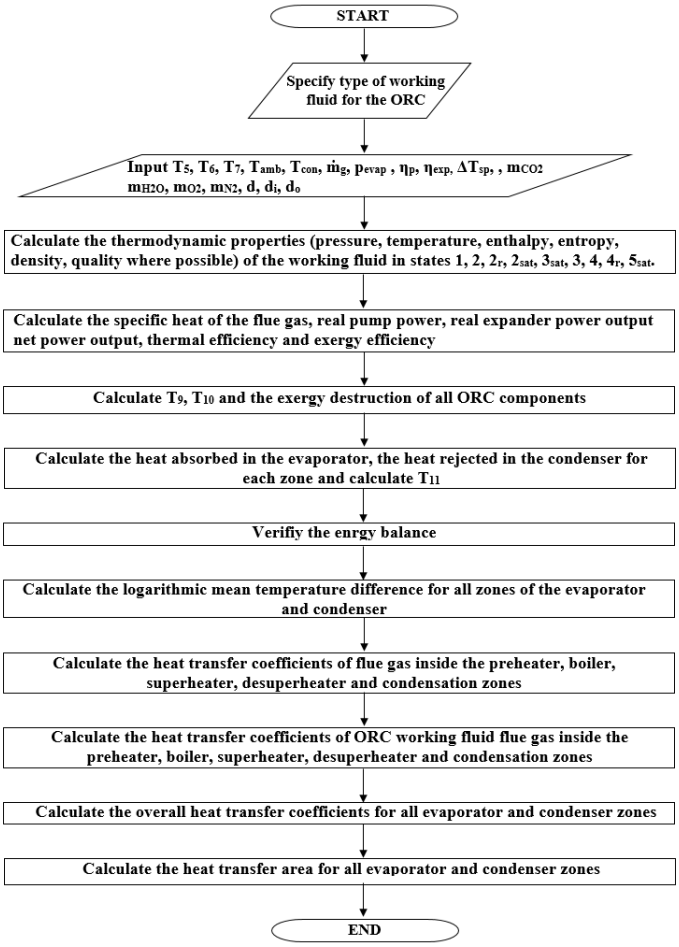

Figure 5. Flow chart of the EES program.

Table 1. Validation of the results with data published in [8].

	$\eta_{th,ORC}\,[-]$	$v_{4r}/v_3\,[-]$	$A_{tot}/P_{net,ORC}\,[m^2/kW]$	**Source**
R245fa	0.123	14.0	0.50	[8]
	0.125	14.3	0.49	Present
R134a	0.075	3.3	0.80	[8]
	0.080	3.3	0.77	Present

In [8], both evaporator and condenser are plate type heat exchangers while in present work the counter-flow double pipe type of heat exchanger are considered. Details about the geometry of the heat exchangers considered in the present work can be found in [3]. In this situation, even if the equations that are used to compute the heat transfer coefficients are different, the value obtained for the total heat transfer area per net power output can be used to validate the results obtained in the present work for the heat transfer areas of evaporator and condenser. Table 1 shows very good

agreement between the results obtained in the present work and the ones from [8] for both working fluids.

The results obtained in the present work have been compared for benzene and R134a working fluids, as shown in Table 2, with the ones reported in [8] and [9]. The input data used to generate the results from Table 2 is: flue gas composition in terms of mass fractions – $m_{CO2} = 9.1\%$, $m_{H2O} = 7.4\%$, $m_{N2} = 74.2\%$, $m_{O2} = 9.3\%$, temperature of the flue gas at the evaporator inlet $T_5 = 743.15\ K$, temperature of the flue gas at the evaporator outlet (form the condition of avoiding condensation) $T_6 = 393.15\ K$, flue gas mass flow rate $\dot{m}_g = 15673\ kg/h$, temperature of the ORC-based system working fluid at the expander inlet has been considered $T_3 = 494.7\ K$ in case of benzene and $T_3 = 374.9\ K$, evaporating pressure $p_{evap} = 2000\ kPa$ in case of benzene and $p_{evap} = 3723.4\ kPa$ in case of R134a, as reported in [9], expander efficiency $\eta_{exp} = 0.7$, pump efficiency $\eta_p = 0.8$. The results presented in Table 2 for the present work have been obtained by imposing a minimum superheating increment $\Delta T_{sp} = 0{,}1\ K$ in case of benzene and $\Delta T_{sp} = 5\ K$ in case of R134a. This superheating increments have been imposed in order to ensure the operation of the EES program developed as described in Figure 5. The results that are compared in Table 2 are: net power output of the ORC-based system $P_{net,ORC}\ [kW]$, thermal efficiency of the ORC-based system $\eta_{th,ORC}\ [-]$, condensing pressure $p_{con}[kPa]$, evaporating pressure $p_{evap}\ [kPa]$, evaporating temperature $T_{evap}\ [K]$, ORC-based system working fluid mass flow rate $\dot{m}_{ref}\ [kg/s]$, ORC-based system working fluid flow rate (at the expander inlet) $\dot{V}_{ref}\ [m^3/s]$, expansion ratio $v_{4r}/v_3\ [-]$ and $\Delta h_{3-4r}\ [kJ/kg]$.

Table 2. Validation of the results with data published in [8] and [9].

	$P_{net,ORC}$ $[kW]$	$\eta_{th,ORC}$ $[-]$	p_{con} $[kPa]$	p_{evap} $[kPa]$	T_{evap} $[K]$	$\dot{m}_{ref}$ $[kg/s]$	$\dot{V}_{ref}$ $[m^3/s]$	v_{4r}/v_3 $[-]$	Δh_{3-4r} $[kJ/kg]$	**Source**
Benzene	349.3	0.199	19.6	2000	494.5	2.737	0.052	107.0	130.5	[9]
	334.1	0.198	19.6	2000	494.5	2.560	0.049	107.3	130.5	[8]
	341.2	0.198	19.8	2000	494.6	2.676	0.051	107.1	130.4	Present
R134a	147.5	0.085	883.3	3723.4	369.9	8.967	0.041	5	19.4	[9]
	159.7	0.079	883.8	3723.4	369.9	9.917	0.034	6.2	16.1	[8]
	142.9	0.083	887.5	3723.4	369.9	9.367	0.040	5.42	18.3	Present

Table 2 shows good agreement between the results obtained in the present work and the ones from [8] and [9] for both working fluids. Some differences between the results can be noticed mainly due to (i) the fact that in [8] the EES (Equation Evaluation Solution) data base is used, in [9] REFPROP data base is used while in the present work the data base available in EES (Engineering Equation Solver) is used and (ii) because in the present work a minimum superheating increment has been considered that enables the use of the program flow chart presented in Figure 5.

5. Mathematical model implementation. Working fluid selection

The mathematical model can be implemented according to the flow chart described in Figure 5 and it corresponds to the design activity of an ORC-based system for a given type of heat source. In this section the focus will be on the selection of the working fluid. In the present work the type of heat source is flue gas from a 4-stroke, 4-cylinder ICE that drives an electric generator for which the main technical data for full operation load is presented in Table 3. Full load means that the electric generator is operating at full capacity (the electricity demand is 36 kWe) that implies full load operation of the ICE (about 37.7 kW). A description of the experimental setup and data for partial load operation is given in [3].

Table 3. Main technical data of the internal combustion engine.

Engine Power	37.7	kW
Electrical power output	36	kWe
Engine speed	1500	rot/min
Piston stroke	110	mm
Cylinder diameter	98	mm
Compression ratio	18:1	-
Flue gas temperature	753	K
Flue gas mass flow rate	192	kg/h
Combustion air mass flow	183.5	kg/h
Fuel consumption	8.5	kg/h

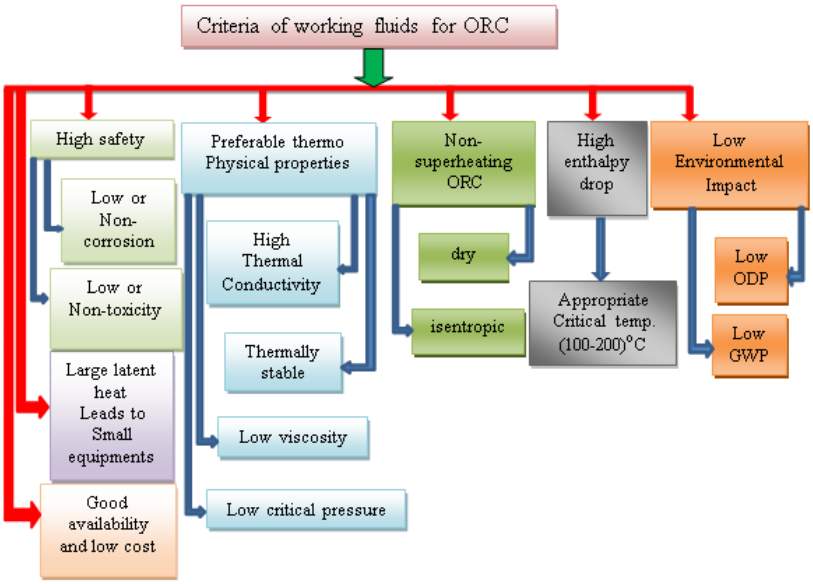

Figure 6. Selection criteria of organic fluids used in ORC.

Many scientific publications deal with the selection of working fluids. Most often, these works propose a comparison between a set of candidate working fluids in terms of thermodynamic performance and based on a thermodynamic model of the ORC cycle. An optimization must be performed for each screened medium, because the optimal working conditions are closely linked to the selected working fluid. Choosing the right working fluid to use in ORC depends on many factors, therefore it is not an easy task. The criteria shown in Figure 6 should be taken into consideration in order to figure out the best candidates.

As mentioned in Section 2, there are three types of working fluids for ORC systems, namely: "wet", "isentropic" and "dry" [10]. "Wet" working fluids have a negative slope of the dry saturated vapor curve (Figure 1 a)), "isentropic" have an infinite slope of the dry saturated vapor curve (Figure 1 b) and "dry" fluids have a positive slope of the dry saturated vapor curve (Figure 1 b)) [10]. The slope of the dry saturated vapor curve ds/dT can be computed using the formula (21) proposed in [10-12]:

$$\frac{ds}{dT}=\frac{T_{evap}\cdot c_p-\Delta h_{evap}\cdot\left(\frac{n\cdot T_{r,evap}}{1-T_{r,evap}}+1\right)}{T_{evap}^{\ 2}}. \tag{21}$$

In relationship (21), the following notations have been used: $T_{evap}\left[K\right]$ is the evaporating temperature, $c_p\left[kJ/(kg\ K)\right]$ is the specific heat of the dry saturated vapor at evaporation conditions, $\Delta h_{evap}\left[kJ/kg\right]$ is the latent heat of evaporation corresponding to the evaporating pressure, n is an exponent which, according to [10-12], can take the values 0.375 or 0.38 (for the present work the value of 0.38 has been chosen) and $T_{r,evap}$ is the reduced evaporating temperature and can be computed as:

$$T_{r,evap}=\frac{T_{evap}}{T_{cr}}. \tag{22}$$

In relationship (22), $T_{cr}\left[K\right]$ is the critical temperature of the working fluid.

The working fluids for which the absolute value of ds/dT is less than 0.5, they are considered to be isentropic.

The most appropriate working fluid for the ORC systems can be determined using the properties presented in Table 4 in correlation with the properties presented in Figure 6 and the working fluid type provided by relationship (21). For the present study the following working fluids have been screened: R134a, R236fa, R245fa from hydrofluorocarbons (HFCs) [10, 13], R1234yf and R1234ze (R1234ze[E] in the EES data base) from hydrofluoroolefines (HFOs) group [13], R290 (propane), R600 (butane), R600a (isobutane), pentane, hexane, benzene and toluene from hydrocarbons (HCs) group [10, 13], RC318 from perfluorocarbons (PFCs) group [13] and HFE7100 and HFE7500 from hydrofluoroethers (HFEs) group [13]. The last two columns of Table 4 present the net power output ($P_{net,ORC}$) and thermal efficiency ($\eta_{th,ORC}$) of the ORC-based system computed with the program presented in Figure 5.

All properties and results presented in Table 4, except the values for ODP and GWP 100yr, have been obtained using the EES software [5] considering the following input data corresponding to the full load operation of the electric generator [3]: flue gas composition in terms of mass fractions – $m_{CO2}=9.1\%$, $m_{H2O}=7.4\%$, $m_{N2}=74.2\%$, $m_{O2}=9.3\%$ [3,14], temperature of the flue gas at the evaporator inlet $T_5=743.15\ K$, temperature of the flue gas at the evaporator outlet (form the condition of avoiding condensation) $T_6=413.15\ K$, flue gas mass flow rate $\dot{m}_g=192\ kg/h$, evaporating temperature $T_{evap}=363\ K$, temperature of the ORC-based system working fluid at the expander inlet

has been determined considering the same superheating increment of $\Delta T_{sp} = 30\ K$ for all screened working fluids, condensing temperature $T_{con} = 293.15\ K$, expander efficiency $\eta_{exp} = 0.7$ and pump efficiency $\eta_p = 0.8$. The values for the T_{cr} [K] and p_{cr} [kPa] can give the reader a quick image of the temperature and pressure ranges in which a working fluid can be used. The value for the evaporating temperature have been chosen to suit all working fluids and to be lower than the critical temperature. The ozone depleting potential (ODP) and global warming potential for 100 years (GWP 100yr) are the environmental factors taken into consideration into present work. For all screened working fluids the ODP is zero, while GWP 100yr has different values. Also, safety factors have been considered, according to ASHRAE [15].

Table 4. Properties of the screened working fluids.

Working fluid	T_{cr} [K]	p_{cr} [kPa]	Δh_{evap} [kJ/kg]	c_p [kJ/(kgK)]	ODP	GWP_{100yr}	ASHRAE Safety group	Group	ds/dT	Type	$P_{net,ORC}$ [kW]	$\eta_{th,ORC}$ [-]
R134a	374.20	4059	82.79	3.11	0 [15]	1300 [10, 15]	A1 [10, 15]	HFC	0.21	Isen.	1.68	0.084
R236fa	398.10	3200	95.95	1.335	0 [15]	9810 [13, 15]	A1 [13, 15]	HFC	0.084	Isen.	1.61	0.081
R245fa	427.20	3651	144.00	1.272	0 [15]	1030 [12, 15]	B1 [13, 15]	HFC	0.063	Isen.	1.72	0.086
R1234yf	367.90	3382	51.44	5.395	0 [15]	4 [13, 15]	A2L [13, 15]	HFO	3.369	Dry	1.565	0.078
R1234ze	382.5	3632	92.11	2.118	0 [15]	6 13, 15]	A2L [13, 15]	HFO	0.194	Isen.	1.637	0.082
R290	369.80	4247	134.30	8.763	0 [15]	0 [13] ~ 20 [15]	A3 [13, 15]	HC	2.52	Dry	1.637	0.082
R600	425.10	3796	276.90	2.453	0 [15]	0 [13] ~ 20 [15]	A3 [13, 15]	HC	- 0.0096	Isen.	1.709	0.085
R600a	407.8	3640	233.4	2.668	0 [15]	0 [13] ~ 20 [15]	A3 [13, 15]	HC	0.13	Isen.	1.662	0.083
RC318	388.4	2778	63.11	1.247	0	10300 [13]	A1 [13, 15]	PFC	0.354	Isen.	1.452	0.073
HFE7100	468.5	2229	105.30	1.015	0	297 [13]	- [13]	HFE	0.951	Dry	1.525	0.076
HFE7500	534.2	1550	100.20	0.994	0	- [13]	- [13]	HFE	1.365	Dry	1.464	0.074

In order to choose the most suitable working fluids for the ORC system among the ones presented in Table 4, a selection procedure is presented next, based on four main screening criteria that can be applied in the following order: environmental, safety, technical and economic. The screening criteria has been presented in this order because, lately, it seems that environmental and safety criteria are of greater influence than the technical and economical ones. The environmental criteria can be applied in correlation with Regulation (EU) No 517/2014 of the European Parliament and of the Council of 16 April 2014 on fluorinated greenhouse gases and repealing Regulation (EC) No 842/2006 [16], which stipulates that by 2030 the HFCs that have a GWP higher that 2500 are subjected to severe restrictions. If this stipulation is applied to screen the fluids from Table 4, even if they are not HFCs, R236fa and RC318 are eliminated.

The safety criteria should follow the definition presented in [16] which says that there are six safety groups related to toxicity and flammability, namely: A1, A2, A3, B1, B2 and B3. According to the same source [16] the least hazardous fluids belong to group A1 and the most hazardous ones to group B3. Also, it is important to mention that fluids from group A have lower toxicity while the ones from group B have higher toxicity. The numbers following the letters, 1,2, 2L and 3 denote the flammability level, 1 being the lowest one. For the remaining candidates, if the second safety criterion is applied,

fluids from group A3 and B1 should be eliminated due their high flammability level and toxicity, respectively. In these condition, the eliminated fluids are R245fa, R290, R600 and R600a. After applying the first two screening criteria the reaming candidates are: R134a, R1234yf, R1234ze, HFE7100 and HFE7500. For these fluids, the technical screening criteria can be applied.

The technical criteria, in the present work, refers to the values obtained for the net power output and thermal efficiency of the ORC-based system. The candidates showing the lowest values for the net power output and thermal efficiency are eliminated. These fluids are: HFE7100 and HFE7500. After applying the first three screening criteria, the remaining candidates are R134a, R1234yf and R1234ze. Among these, the one displaying the highest values for the net power output and thermal efficiency is R134a, followed by R1234ze and R1234yf.

The final criterion that could be applied is the economical one and it refers mainly to the cost of one kilogram of working fluid. This criterion has not been taken into consideration in the present work. In this conditions, the most suitable working fluids established after screening the fluids from Table 4 are R134a, R1234ze and R1234yf.

As it can be noticed from Table 4, R134a and R1234ze are isentropic working fluids and R1234yf is a dry working fluid. At this point a discussion about the type of working fluid and the use of relationship (21) to determine it is needed. Fluid R134a will be taken as example. The use of relationship (21) in the context of present work and especially for the data used to generate Table 4, indicates fluid R134a as isentropic. For the same working fluid, reference [10] in Table 1 indicated it as wet, reference [13] in Table 1 indicates is as isentropic and [17] in Table 1 indicates it as wet. These results could cause some confusion but in reality the shape of the dry saturated vapor curve is changing depending on the evaporating (saturation) pressure and thus the slope given by relationship (21). For the results presents in Table 4 the evaporating pressure is $p_{evap} = p_{3sat} = 3237\ kPa$ and the result given by relationship (21) $ds/dT = 0.21$ indicating a isentropic fluid. If the calculations are performed for a lower pressure, for example atmospheric pressure of 1013 kPa, the result obtained with relationship (21) is $ds/dT = -2.96$ indicating that R134a is a wet fluid.

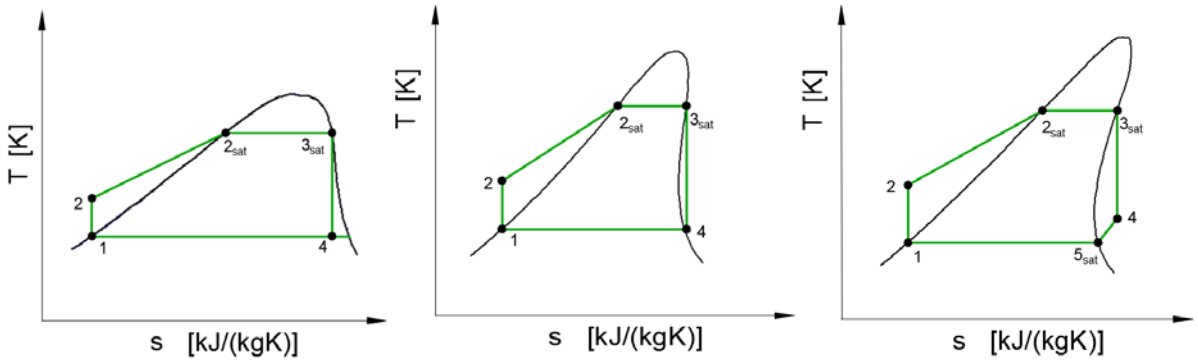

a) b) c)

Figure 7. The thermodynamic cycle in T-s coordinates for the ORC-based system with a configuration similar to the one presented in Figure F1 with no superheating degree a) for "wet" working fluids, b) for "isentropic" working fluids and c) for "dry" working fluids.

When establishing the type of working fluid, one should also take into consideration the state of point 4 at the expander outlet for an ORC-based with a configuration similar to the one in Figure 1 with no superheating degree, as presented in Figure 7 a), b) and c). Figure 7 a), b) and c) present the thermodynamic cycle of an ORC-based system with no superheating degree for the same situations as presented in Figure 2 a), b) and c).

As it can be seen from Figure 7 a), b) and c), in case of wet working fluids the expander outlet state (point 4) is in two-phase region, for isentropic working fluids the expander outlet state (point 4) is very

close to the dry saturated vapour curve and in case of dry working fluids the expander outlet state (point 4) is in superheated vapour region.

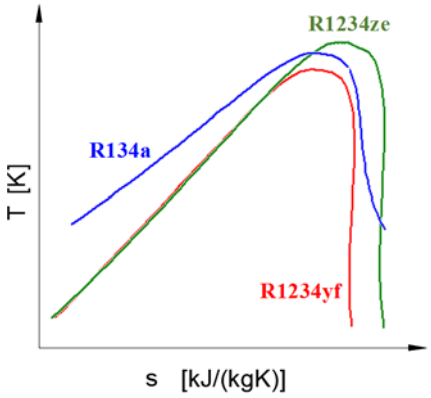

Figure 8. The shape of saturation curves for the three selected fluids R134a, R1234yf and R1234ze.

If this additional way of establishing the type of working fluid is taken into consideration, the fluids established in the present paper as being the most suitable ones are R134a wet, R1234ze isentropic and R1234yf also isentropic. The shape of the saturation curves for these three selected fluids, generated with EES software [5] is presented in Figure 8.

In future work, the calculation will be performed for the three working fluids from Figure 8.

In general, for ORC-based systems which are designed to operate with no superheating, dry and isentropic fluids are preferred. Nevertheless, if isentropic and wet fluids are used, then superheating is recommended to avoid the possibility of expander damaging when the outlet state 4 is in the two-phase zone.

6. Conclusions

The present paper deals with working fluid selection procedure for ORC systems used for waste heat recovery from an internal combustion engine that drives a stationary electric generator. Due to its ability to operate with low temperature level the ORC technology is suitable for WHR from flue gas of ICE. The ORC-based heat recovery system is composed of expander, condenser, evaporator, working fluid pump. The mathematical modelling of the ORC-based system is a continuation of previous work conducted by the authors. The assumptions adopted for the development of the mathematical model are: (i) negligible heat loss in pipes and equipment; (ii) negligible pressure drops in pipes and equipment; (iii) flue gas is non-condensable; (iv) steady state operation. For the mathematical model described in the present work, a program has been developed in Engineering Equation Solver – EES. For the validation of the mathematical model, input data available in literature for similar work has been used. The results show very good agreement.

The mathematical model has been implemented using data available for 4-stroke, 4-cylinder ICE that drives an electric generator for which the main technical data for full operation load have been presented.

A selection procedure for the ORC-based system working fluid is proposed. First, a discussion about the available working fluid type is conducted based on the derivative ds/dT. Secondly, fifteen working fluid candidates have been screened based on environmental, safety and technical criteria. The screened fluids are: R134a, R236fa, R245fa, R1234yf, R1234ze, R290, R600, R600a, pentane, hexane, benzene, toluene, RC318, HFE7100 and HFE7500. The screening criteria has been applied in a specific order: environmental, safety and technical, as the first two tend to be of greater importance than the las one. After applying the environmental criterion, the eliminated candidates are R236fa and RC318. If the second criterion is applied, the eliminated candidates are: R245fa, R290, R600 and R600a. The technical criteria, in the present work, refers to the values obtained for the net power

output and thermal efficiency of the ORC-based system. After applying the technical criterion, the remaining candidates are R134a, R1234yf and R1234ze. The highest values for the net power output and thermal efficiency are achieved using R134a, followed by R1234ze and R1234yf. The economical criterion involving the cost associated to each fluid has not been considered in the present work.
In the las part of the work a discussion about the type of working fluid and the use of the derivative ds/dT to determine it, was carried out. It is pointed out that using the ds/dT to define a fluid as "wet", "isentropic" and "dry" can lead to some understanding difficulties because it is highly sensitive to the pressure level. Fluid R134a has been taken as an example. In the present work, R134a is indicated as "isentropic" fluid while in other similar work it is indicated as "wet". These results could cause some confusion, but in reality the shape of the dry saturated vapor curve is changing depending on the evaporating (saturation) pressure and thus the slope given by ds/dT . For the results presents in the present work, evaporating pressure is $p_{evap} = p_{3sat} = 3237\ kPa$ and the result given by derivative ds/dT is $ds/dT = 0.21$ indicating a isentropic fluid. If the calculations are performed for a lower pressure, for example atmospheric pressure of 1013 kPa, the result obtained with the derivative ds/dT is $ds/dT = -2.96$ indicating that R134a is a wet fluid. Taking these into consideration, when establishing the type of working fluid, one should also take into consideration the state of working fluid at the expander outlet for an ORC-based with no superheating degree. In case of wet working fluids, the expander outlet state is in two-phase region, for isentropic working fluids the expander outlet state is very close to the dry saturated vapour curve and in case of dry working fluids the expander outlet state is in superheated vapour region. If this additional way of establishing the type of working fluid is taken into consideration, the fluids established in the present paper as being the most suitable ones are R134a wet, R1234ze isentropic and R1234yf also isentropic.

Future work will focus on using the mathematical model and the three working fluid candidates to design the ORC-based system.

7. References

[1] Sprouse C and Depcik C 2013 Review of organic Rankine cycles for internal combustion engine exhaust waste heat recovery *Applied Thermal Engineering* **51** pp 711-722
[2] Taban D, Dobrovicescu A, Apostol V and Pop H 2017 Current state of research in the field of waste heat recovery from internal combustion engines Report I – Doctoral thesis
[3] Badescu V, Aboaltabooq M H K, Pop H, Apostol V, Prisecaru M and Prisecaru T 2017 Design and operational procedures for ORC-based systems coupled with internal combustion engines driving electrical generators at full and partial load *Energy Conversion and Management* **139** pp 206–221
[4] Apostol V, Pop H, Dobrovicescu A, Prisecaru T, Alexandru A and Prisecaru M 2015 Thermodynamic Analysis of ORC Configurations Used for WHR from a Turbocharged Diesel Engine *Procedia Engineering* **100** pp 549–558
[5] Engineering Equation Solver 2017 Academic commercial V.10.111-3D #4487 Faculty of Mechanical Engineering University Politehnica of Bucharest
[6] Mago P J, Chamra L M and Somayaji C 2006 Performance analysis of different working fluids for use in organic Rankine cycles *Proc. IMechE, Part A: J. Power and Energy* **221** pp 255-264
[7] Deaconu A S, Chirilă, A I Năvrăpescu, V Ghiţă C and Deaconu I D 2013 Thermal analysis of a PMSM for an intermittent periodic duty cycle *The 8TH International Symposium On Advanced Topics in Electrical Engineering (ATEE 2013)* p 16
[8] Tian H, Shu G, Wei H, Liang X and Liu L 2012 Fluids and parameters optimization for the organic Rankine cycles (ORCs) used in exhaust heat recovery of Internal Combustion Engine (ICE) *Energy* **47** pp 125-136
[9] Iacopo V and Agostino G 2010 Internal combustion engine (ICE) bottoming with organic

Rankine cycles (ORCs) *Energy* **35** pp 1084-93
[10] Zhang T, Zhu T, An W, Song X, Liu L and Liu H 2016 Unsteady analysis of a bottoming Organic Rankine Cycle for exhaust heat recovery from an Internal Combustion Engine using Monte Carlo simulation *Energy Conversion and Management* **124** pp 357–368
[11] Liu B T, Chien K H and Wang C C 2014 Effect of working fluids on organic Rankine cycle for waste heat recovery *Energy* **29(8)** pp1207–17
[12] Poling B E, Prausnitz J M and O'Connell JP 2001 *The properties of gases and liquids* (McGraw-Hill).
[13] Vivian J, Manente G and Lazzaretto A 2015 A general framework to select working fluid and configuration of ORCs for low-to-medium temperature heat sources *Applied Energy* 156 pp 727–746.
[14] Junjiang B and Li Z 2013 A review of working fluid and expander selections for organic Rankine cycle *Renew Sustain Energy Rev* **24** pp 325–342
[15] ASHRAE Handbook Fundamentals 2013 SI Edition
[16] Regulation (EU) No 517/2014 of the European Parliament and of the Council of 16 April 2014 on fluorinated greenhouse gases and repealing Regulation (EC) No 842/2006
[17] Satanphol K, Pridasawas W and Suphanit B 2017 A study on optimal composition of zeotropic working fluid in an Organic Rankine Cycle (ORC) for low grade heat recovery *Energy* **123** pp 326-339

Acknowledgments
The authors gratefully acknowledge the support provided by Executive Agency for Higher Education, Research, Development and Innovation Funding of Romania. Through the Program PN-II-PT PCCA-2011-3.2-0059, Grant No.: 75/2012.